Genes & Diseases (2022) 9, 797–806

Available online at www.sciencedirect.com

ScienceDirect

journal homepage: http://ees.elsevier.com/gendis/default.asp

FULL LENGTH ARTICLE

Vitamin D receptor (VDR) contributes to the development of hypercalciuria by sensitizing VDR target genes to vitamin D in a genetic hypercalciuric stone-forming (GHS) rat model

Shang Guo [a], Weekai Chia [a], Hongwei Wang [b], David A. Bushinsky [c], Biao Zhong [a,*], Murray J. Favus [d,**]

[a] *Department of Orthopedics, Shanghai Jiaotong University Affiliated Sixth People's Hospital, Shanghai 200233, PR China*
[b] *Shanghai Realgen Biotech Co., Ltd, Shanghai 200215, PR China*
[c] *Department of Nephrology, Pharmacology and Physiology, University of Rochester, Rochester, NY 14642, USA*
[d] *Section of Endocrinology, Department of Medicine, University of Chicago, Chicago, IL 60637, USA*

Received 12 April 2020; received in revised form 8 September 2020; accepted 9 September 2020
Available online 30 September 2020

KEYWORDS
Acetylation;
ChIP;
GHS;
Methylation;
Snail;
VDR;
VDR target Gene

Abstract Human idiopathic hypercalciuria (IH) is the most common cause of calcium oxalate nephrolithiasis with perturbed calcium metabolism with increased bone resorption and decreased renal calcium reabsorption, which can be phenotype-copied in the genetic hypercalciuric stone-forming (GHS) rat model. We previously demonstrated that high VDR expression plays important roles in the development of hypercalciuria in the GHS rats. However, the underlying mechanism through which VDR impact hypercalciuria development remains to be fully understood. Here, we sought to determine how VDR regulated its target genes that are implicated in calcium homeostasis and potentially hypercalciuria. We found that VDR expression in the GHS rats was elevated in the calcium transporting tissues, as well as in the thymus and prostate, but not in lung, brain, heart, liver and spleen, when compared with control SD rats. Snail expression in the GHS rats was significantly downregulated in kidney, intestine, thymus and testis. Intraperitoneal injection of $1,25(OH)_2D_3$ significantly upregulated the expression of renal calcium sensing receptor (CaSR), intestinal calcium transporters transient receptor

* Corresponding author.
** Corresponding author. Section of Endocrinology, Department of Medicine, University of Chicago Pritzker School of Medicine, 5841 S. Maryland Ave. MC 1027, Chicago, IL 60637, USA.
E-mail addresses: biao.zhong@139.com (B. Zhong), mjfavus@gmail.com (M.J. Favus).
Peer review under responsibility of Chongqing Medical University.

https://doi.org/10.1016/j.gendis.2020.09.001

potential vanilloid type 6 (TRPV6), and VDR in GHS rats, compared with that in control SD rats. ChIP assays revealed that VDR specifically bound to the proximal promoters of target genes, followed by histone H3 hyperacetylation or hypermethylation. Collectively, our results suggest that elevated VDR expression may contribute to the development of hypercalciuria by sensitizing VDR target genes to $1,25(OH)_2D_3$ through histone modifications at their promoter regions in a genetic hypercalciuric stone-forming (GHS) rat model.

Introduction

Human idiopathic hypercalciuria (IH), the most common cause of calcium oxalate nephrolithiasis, and GHS rats exhibit similar changes in Ca metabolism, including increased bone resorption and decreased renal calcium reabsorption.[1–6] Our previous studies have found that higher VDR expression levels in the intestine, kidney, and bone play important roles in hypercalciuria in GHS rats.[4,5,7,8] The lengthy *in vivo* half-life of VDR mRNA and protein can partially explain the high VDR expression in GHS rats.[7,9] Snail is a transcriptional repressor of the VDR gene.[10] Our recent data show that Snail downregulates VDR transcription and expression by binding to multiple E-boxes in the VDR promoter regions and deacetylating histones H3 and H4; more interestingly, Snail inversely correlates with VDR in the intestine and kidney at the mRNA and protein levels.[11] These data strongly suggest that Snail plays an important role in the VDR levels being high, as they relate to Ca transport and metabolism in GHS rats.

VDR is an essential nuclear receptor that has been reported to function in Ca homeostasis, the immune system, and cell proliferation and differentiation.[12–14] VDR exerts its biological effects by regulating gene expression. The $1,25(OH)_2D_3$ level *in vivo* is tightly controlled by several cytochrome P450 (CYP) family enzymes, such as CYP24 and CYP27B1.[15,16] CYP24 was found in the kidney, intestine, and bone and can hydroxylate 25-OH-D_3 or $1,25(OH)_2D_3$ into $24,25(OH)_2D_3$ and $1,24,25(OH)_3D_3$.[15] This process is believed to be the first step in degrading and maintaining appropriate active $1,25(OH)_2D_3$ levels *in vivo*.[16] CYP27B1 is another enzyme that promotes the synthesis of $1,25(OH)_2D_3$, which it does by catalyzing 25-OH D_3 into $1,25(OH)_2D_3$.[14] $1,25(OH)_2D_3$ can modulate CYP24 and CYP27B1 expression, and the detailed regulatory mechanisms responsible for this regulation have been discovered *in vitro*.[16–19] However, the detailed mechanisms of how $1,25(OH)_2D_3$ up- and downregulates CYP24 and CYP27B1 expression *in vivo* are not clear, especially in our GHS rat model. Our previous data indicated that VDR gene expression is hypersensitive to $1,25(OH)_2D_3$ administration in GHS rats[7]; however, whether VDR target genes CYP24 and CYP27B1 are hyperresponsive to $1,25(OH)_2D_3$ remains unknown.

GHS rats are characterized by defects in Ca transport and metabolism.[1] High VDR levels are associated with hypercalciuria in GHS rats. Elevated VDR levels mediate the upregulation of Ca transport and reabsorption genes such as 9- and 28-kDa calbindins and CaSR in the small intestine and kidney, contributing to hypercalciuria and stone formation in GHS rats.[8,9] CaSR is a VDR target gene and is expressed in various tissues, including the kidney.[20,21] VDR can upregulate CaSR expression by binding to its promoter.[21] However, how VDR activates CaSR expression *in vivo* is not completely understood. TRPV6 is an epithelial Ca channel that is mainly expressed in the intestine and is responsive to intestinal Ca absorption.[22] TRPV6 knockout mice showed a 60% decrease in intestinal Ca absorption.[23] Therefore, the role of TRPV6 in hypercalciuria and how $1,25(OH)_2D_3$ upregulates its expression in GHS rats remain to be explored.

VDR regulates target gene expression through interaction with the retinoid X receptor (RXR) and through recruiting coregulators to target gene promoter regions, modifying histone state and chromatin structure, which results in gene up- or downregulation.[24,25] Therefore, this study was designed to test whether VDR modulates target gene expression through promoter binding and histone modification in GHS rats.

Material and methods

Animals models

A GHS rats colony was created by the selective breeding of male and female Sprague–Dawley rats (S-D, Harlan, Inc., Indianapolis, IN) with spontaneous hypercalciuria.[2] Beyond the 65th generation, GHS rats have consistently excreted 8–10 times the level of urine calcium that is excreted by wild-type normocalciuric (NC) SD rats. Male and female GHS rats were raised at the University of Rochester and were shipped to the University of Chicago at 6–7 weeks of age and with a body weight of 260–280 g. SD rats purchased from Harlan, Inc. Indianapolis were matched with the GHS rats based on age and body weight. All animal experiments were approved by the University of Chicago Institutional Animal Care and Use Committee.

Western blots

Tissue was homogenized in cold PBS buffer with a protein inhibitor cocktail. The mix was vortexed at full speed for 20s at 5 min intervals and then centrifuged for 15 min at $14,000\times g$ at 4 °C. The supernatant was removed and stored at −80 °C. Protein concentration was determined using the Bio-Rad protein assay (Bio-Rad, Hercules, CA).

Aliquots of total protein (20 μg) were denatured in 6x SDS sample buffer (7 ml 4x Tris/HCl, SDS [pH 6.8], 3.0 ml of glycerol, 1 g of SDS, 0.93 g of dithiothreitol, and 1.2 mg of bromophenol blue in 10 ml of distilled deionized H_2O) and then loaded onto SDS denaturing gels for discontinuous electrophoresis. The proteins were transferred onto polyvinylidene difluoride membranes (Immobilon-P; Millipore, Bedford, MA) by electroblotting at 90 V for 1 h. The membranes were then blocked with 5% nonfat dried milk in TBS that contained 0.1% Tween-20 (TBS-T). A primary antibody was diluted with 3% nonfat dried milk in TBS-T. Then, the membrane was incubated with the diluted primary antibody at room temperature for one hr. Membranes were washed with TBS-T and incubated with horseradish peroxidase-conjugated anti-rat IgG for one hr at room temperature. Protein bands were developed using an ECL Chemiluminescence System (Amersham Life Science, Buckinghamshire, UK). The blots were quantified with One-Scan 1-D gel Analysis software (Scanalytics Inc., Fairfax, VA).

Real-time PCR

Female GHS rats were IP injected with 200 ng/kg BW $1,25(OH)_2D_3$ or with ethanol (as a control). Twelve hours later, RNA was isolated from the kidneys and intestines from both groups using TRIzol, and cDNA was subsequently synthesized using a High Capacity cDNA Reverse Transcription Kit (Applied Biosystems, Foster City, CA) according to the manufacturer's directions. The primer sequences for rat CYP24, CYP27, VDR, CaSR, TRPV6 and GAPDH were as follows: CYP24 (forward) 5′-GATCCTGGAAGGACAGGAGT-3′, (reverse) 5′-GGAAGTCAGCCAAGACCTCA-3'; CYP27 (forward) 5′-AAAGGTGTCTGTCCAGTCCA-3′, (reverse) 5′-CTCATAGAGTGCCCAGGAGA-3'; VDR (forward) 5′-TGTTCACCTGTCCCTTCAAT-3′, (reverse) 5′-CGCTGTACCTCCTCATCTGT-3'; CaSR (forward) 5′-GTGGAGAGACAGATGCGAGT-3′, (reverse) 5′-TGCAAGAAGTGTGGTTCTCA-3'; TRPV6 (forward) 5′-GATGGCTGTGGTAATCTTGG-3′, (reverse) 5′-ATCGATGATGGTGAGGAAGA-3'; and GAPDH (forward) 5′-GCACAGTCAAGGCTGAGAAT-3′, (reverse) 5′-TGAAGACGCCAGTAGACTCC-3'. Quantification of the PCR products was performed using the comparative cycle threshold (Ct) method, as described previously.[26,27] GAPDH was used as an internal control. Statistical analysis was performed using Student's *t*-tests for unpaired comparisons. Data are presented as the means ± SE, and $P < 0.05$ was considered significant.

Tissue ChIP assays

For tissue ChIP assays, frozen intestine and kidney tissues from GHS rats injected with either $1,25(OH)_2D_3$ or a vehicle were thawed at room temperature, cut to generate 1 mm slices, and crossed-linked in 1.5% formaldehyde for 15 min. Tissues were then homogenized with Tissuemiser (Fisher Scientific, Pittsburgh, PA), and the cell suspension was centrifuged at 14,000 rpm for 10 min. SDS lysis buffer was added to the pellets, which were then subjected to sonication. Anti-VDR and acetylated H3 antibodies were used to immunoprecipitate the DNA and protein complex, and IgG alone was used as a negative control. After overnight incubation with the antibodies, immunocomplexes were collected using 80 μL of protein A agarose beads in a slurry (Upstate Biotechnology, Temecula, CA). The agarose beads were washed twice with the following buffers (Upstate Biotechnology): low salt wash buffer; high salt wash buffer; LiCl wash buffer; and TE buffer. DNA was eluted with 1% SDS and 0.1 M $NaHCO_3$ elution buffer, and then it was subjected to reverse cross-linking, proteinase digestion, and purification using a commercial kit (Qiagene, Valencia, CA). The primers used to amplify the target gene promoters are listed in Table 1. For quantitative ChIP, real-time PCR was performed using the SYBR Green PCR Master Mix Kit to amplify the immunoprecipitated DNA, and data are shown as the percentage of input as described before.[28]

Results

Snail inversely correlated with VDR expression in GHS rats

Our previous data show that VDR is highly expressed in the kidneys, intestines, and bones of GHS rats, which accounts for the hypercalciuria in GHS rats.[4,5,7,8] In this study, we investigated whether VDR expression was higher in various tissues. Western blot results show that compared to SD control rats, VDR is highly expressed GHS rat tissues with high levels of Ca transport and metabolism, such as the intestine, kidney, thymus, and prostate (Fig. 1). However, for the liver, heart, lung, spleen, brain, and uterus, VDR expression was not different between GHS and SD rats (Fig. 1). Snail is a transcription factor that promotes epithelial to mesenchymal transition (EMT).[29] A recent report has shown that Snail is a transcriptional repressor of VDR gene expression and that its levels are inversely correlated with VDR expression in colon cancer cells.[10,29] Here, we investigated Snail expression levels in tissues with higher or normal VDR expression (Fig. 2). Our data indicate that Snail is only detectable in the intestine, kidney, thymus, testis, and brain. More interestingly, Snail is downregulated in the presence of higher VDR levels in tissues such as the intestine, kidney, and thymus in GHS rats compared to SD rats. There was no difference in Snail expression between the brain of GHS and SD rats. These results suggest that Snail is inversely correlated with VDR expression in GHS rat tissues that exhibit high VDR expression.

$1,25(OH)_2D_3$ strongly induces or suppresses target gene transcription in GHS and SD rats

$1,25(OH)_2D_3$ exerts its function through up- or down-regulation of VDR response gene expression.[30] In the current study, the following VDR target genes were investigated: Ca transporters CaSR and TRPV6 and the vitamin D catabolism enzymes CYP24 and CYP27B1 as well

Table 1 Primers for tissue ChIP.

Primer	Start	Sequence
CASR-FW1	−4976	CCTGATTGTAGCCAGACCAGC
CASR-RE1	−4822	AGGACTTGGTAGTAACAGAAC
CASR-FW2	−4595	TTCCTCTTTGAAGAATGCACAC
CASR-RE2	−4447	ATCCTCTATCCCAGTGTACCC
CASR-FW3	−4090	CCAGACGTGTGCAACTACGCT
CASR-RE3	−3938	GCTGTCAGGAAACTCTCTGGG
CASR-FW4	−3850	TTCGCCCGCCAAATAAGCTCT
CASR-RE4	−3703	GGAGAGAGATCTTGGCACCTT
CASR-FW5	−3298	ACCATGTCCTTTCTAGGTACAC
CASR-RE5	−3144	AGAATCTGGACAGGACTTGCT
CASR-FW6	−2567	CAACTGCAGGCACTCTGTTAAC
CASR-RE6	−2417	CTGAGTCTTGGCAACAGAAAG
CASR-FW7	−1810	TGAGGGAGAGTCAGGCTCTGTT
CASR-RE7	−1663	ACCAGTTGAAGAAGCTGCGTC
CASR-FW8	−1265	ACACTATCTCATATCAAGCATC
CASR-RE8	−1115	TACAGAAAAACAAGGGACTGT
CASR-FW9	−949	CCCTATTGAGGGAGTCTTAAGT
CASR-RE9	−797	GCCTCCCAGTTTTCTTAGAAC
CASR-FW10	−502	TGCTGTGCCAGAGCCCGAGAAC
CASR-RE10	−352	TCCAGCGTTGTGTCTGCGGTC
TRPV6-FW1	−4893	GCAGAGTTAGATCAAGGAAGT
TRPV6-RE1	−4748	TGTCCTATGACTAGTTTGTGC
TRPV6-FW2	−4569	AAATGTGCACACATGCATCTC
TRPV6-RE2	−4415	CCCACTCTCTGTTTCTTTTGA
TRPV6-FW3	−4308	AACAGCAGTTGACAGGAGGAAG
TRPV6-RE3	−4161	AGAAATAGGAGTCAGGTGCAG
TRPV6-FW4	−3920	TTTGAACCCAGTGACTGGAAC
TRPV6-RE4	−3769	CAGGAAAATGTCTGTAGGTGG
TRPV6-FW5	−2438	GCAGGACTGGAGTGCATGATGG
TRPV6-RE5	−2288	CAGTTGGGGTGGCTTGGCACT
TRPV6-FW6	−2149	CTCACTCCACAGCATGATACAAG
TRPV6-RE6	−2000	AGGACCTTTGTGCCCATTAAG
TRPV6-FW7	−2039	GCGTCAGACTAACACTTGGCTT
TRPV6-RE7	−1891	TACAGCCCTGAGCAAACAATG
TRPV6-FW8	−1700	CTACAGCAACAATACTACACC
TRPV6-RE8	−1579	TATGTGCTTTCCATGGAACGT
TRPV6-FW9	−1008	TCTCTTTGCCAATTAGAGTGAG
TRPV6-RE9	−858	AGAGCCTAGAAGGCAGTTATT
TRPV6-FW10	−385	AGTTGGTGAGAACTCAGAATCT
TRPV6-RE10	−231	AGGAGAAGGAAAGCAAGAAAG
CYP27B1-FW1	−5031	CCATTTCTTGGGACAAGGAGAG
CYP27B1-RE1	−4884	CAAAGGCCATAGACCCAGAGT
CYP27B1-FW2	−4520	AGGAGCGTGGTGTGTGAGACTG
CYP27B1-RE2	−4366	CCACCACCGCCTAGCTTCATT
CYP27B1-FW3	−4150	CCTGGCTGGTTACTTTATGTTT
CYP27B1-RE3	−3998	GCCTTTAATCCTAAGAATTGG
CYP27B1-FW4	−3660	CCTGTCTCCGCAGTAACGCCAT
CYP27B1-RE4	−3513	GGACAGATGCGCCAACAGGAT
CYP27B1-FW5	−2952	TCAACTGAGGAAGGAAAGAAAG
CYP27B1-RE5	−2799	GCTCATCTTTTTCCAGTCACT
CYP27B1-FW6	−1960	GGGGCCAGAAAAAGGAAGATGGT
CYP27B1-RE6	−1807	ACTCCTCCAGGTTAGTGACTG
CYP27B1-FW7	−1817	CCTGGAGGAGTCTGTAACTGAG
CYP27B1-RE7	−1672	GCCAACCCTCACCTCCTATAC
CYP27B1-FW8	−1669	AAGTGCACATATGCTCGTACA
CYP27B1-RE8	−1524	ATGAAGAAATGTCCTAGGGTC
CYP27B1-FW9	−175	GAGACCCAAAAGCCAGCGAGT
CYP27B1-RE9	−22	CTTCTGCACTTGCCTGAACCC

Table 1 (*continued*)

Primer	Start	Sequence
CYP24A-FW1	−5294	GTCTCGCCAAAACTAAACAAAC
CYP24A-RE1	−5147	TCTAGTGTGGATTTAGAGACC
CYP24A-FW2	−4900	CAACTTCCAGAGCTTGGATGCC
CYP24A-RE2	−4780	GTGTGCCTCGGTGTGAGCCTG
CYP24A-FW3	−4481	ACTTGTTCACAGCCTGTTATTC
CYP24A-RE3	−4327	CATGTTGACCAGTCACTGTTT
CYP24A-FW4	−3829	TTTTCTTTGTTTTAATTCACTGT
CYP24A-RE4	−3675	GTGGAATCCCTAGAGACTTAT
CYP24A-FW5	−3274	CACCACCTTCTGCTCAAGAAAT
CYP24A-RE5	−3128	TGTACTGGGAAACACAAAGCC
CYP24A-FW6	−2858	CATGTCCAGACCTTTCATTAG
CYP24A-RE6	−2713	CTAGAAGAGTTCAGAACACCA
CYP24A-FW7	−1964	GTTTGAGCTAGCCTGGTCTATG
CYP24A-RE7	−1810	GCTTAGTCCATTGTCGCAAAC
CYP24A-FW8	−1718	CCCCCACGCATATACAACAGAG
CYP24A-RE8	−1572	ACCATTTCCCCTTCCCTTCTG
CYP24A-FW9	−1182	CAAATCGGATTGCAGAAGCTTC
CYP24A-RE9	−1029	TTTCCAATGCAAAGCCACCAG
CYP24A-FW10	−837	TGGGCGGTGCGCAAGAAGGAAA
CYP24A-RE10	−692	GGTCTACACAGGTGTGTGTCC
CYP24A-FW11	−267	ACCCGCTGAACCCTGGGCTCGAC
CYP24A-RE11	−119	GCGGGTGTGGGAAGAGGATGG
VDR-FW1	−4950	CATTGTCTGCTGCAGACTTGG
VDR-RE1	−4802	ACACGGTGTCAGTCAGCATGT
VDR-FW2	−4696	GCAATGGAGCCAGAAGGATAC
VDR-RE2	−4549	CTATCCTCCAGAAGCCTATGG
VDR-FW3	−4008	TTCAGTCCAGGGGCTGGGCTACC
VDR-RE3	−3858	AGGTGAGGAGGTGGGAGGGCA
VDR-FW4	−3340	GAGTGCTGTCTGTCTTCCCAT
VDR-RE4	−3187	TCCTAAAAGCAGATCCTTGTC
VDR-FW5	−2789	GGATCTAGCAGATGGTTCCTG
VDR-RE5	−2642	AGGCAGGTGGATCTGTGAGTT
VDR-FW6	−2317	CTGGAGATGGTGGAAAGGGTT
VDR-RE6	−2170	GCATACTCTGTGGTTGGTCCA
VDR-FW7	−1882	AGAGCAGTGTTCTTAATGGTTG
VDR-RE7	−1736	GACTAACGGGCATCATTTCTT
VDR-FW8	−1650	GCTCTGTCTTCAAAGATTGACAC
VDR-RE8	−1496	GGAAGGAAGATAAGCACCAAC
VDR-FW9	−499	AGCGCCCTGCAGGAGAAAGTC
VDR-RE9	−345	CGCCGTGGTTCTACCCAGTCT
VDR-FW10	−199	GTCTCCAAGGCGACAGTGCAG
VDR-RE10	−54	AGAGACTGCTCAGCACCTGGC

as VDR itself. Twelve hours after $1,25(OH)_2D_3$ administration in GHS rats, RNA was isolated from their intestines and kidneys and then was subjected to real-time PCR. $1,25(OH)_2D_3$ increased the transcription of CYP24, CaSR, TRPV6, and VDR by 32.8-, 8.9-, 17- and 4.5-fold in GHS rats and 39.5-, 1.6-, 1.83-, and 2.2-fold in SD rats, respectively (Fig. 3). At the same time, $1,25(OH)_2D_3$ decreased CYP27B1 transcription by 68% in GHS rats and 53% in SD rats (Fig. 3). Our data show that high VDR levels in GHS rats strongly mediated $1,25(OH)_2D_3$ action on target gene expression. CaSR, TRPV6, and VDR are more sensitive to $1,25(OH)_2D_3$ treatment in GHS rats than they are in SD rats.

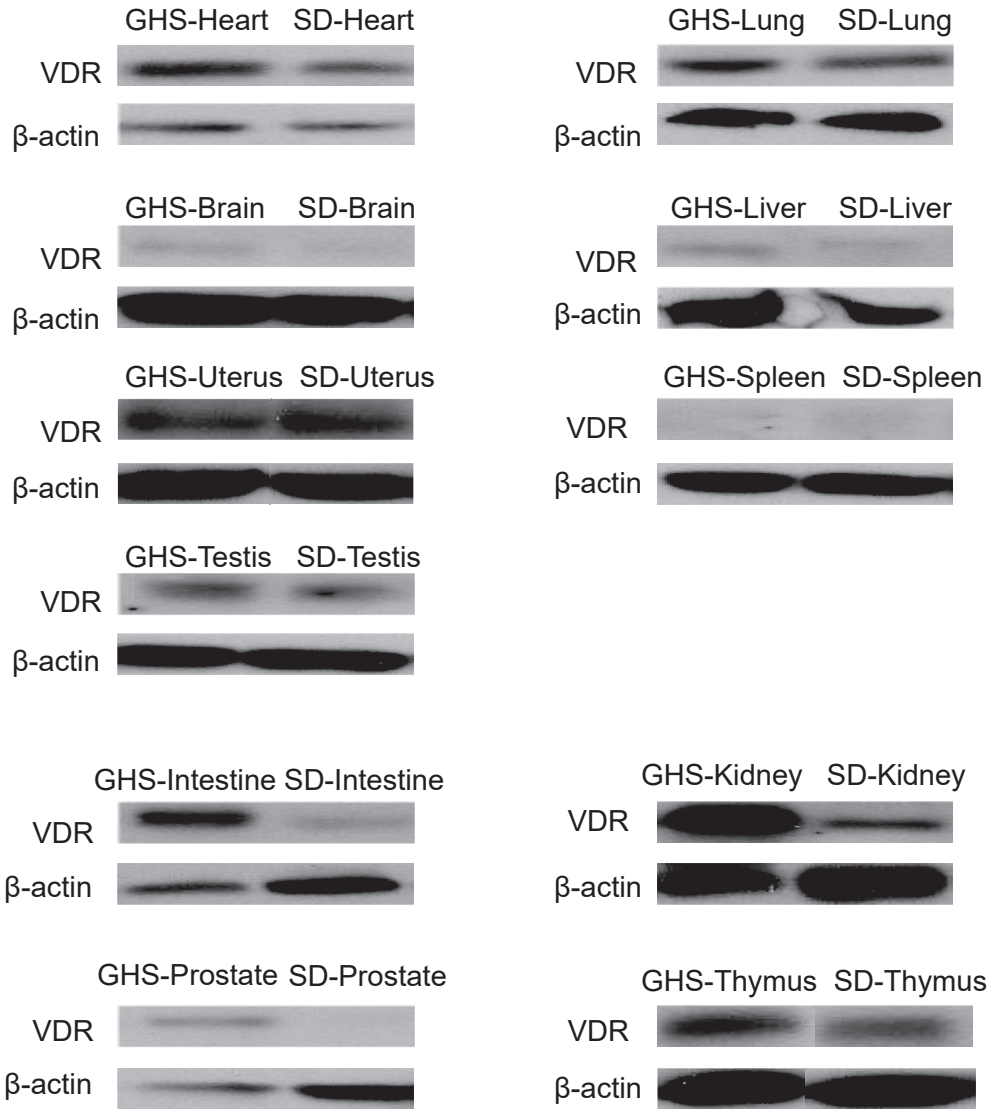

Figure 1 VDR expression in various tissues of GHS and SD rats. Nuclear proteins were isolated from tissues of three GHS rats and SD rats and then were subjected to Western blots using anti-VDR antibodies. Representative data are shown in Figure 1. The expression pattern of VDR in various tissues; VDR is highly expressed in the intestine, kidney, prostate and thymus in GHS rats compared to SD rats.

Hyperacetylation or hypermethylation of histone H3 in multiple regions of the target gene promoter after $1,25(OH)_2D_3$ treatment

Histone acetylation and methylation are associated with gene activation and repression.[31,32] In this study, we investigated whether VDR regulates target gene expression through histone modification. After GHS rats were treated with $1,25(OH)_2D_3$ or vehicle, their intestines and kidneys were harvested and then subjected to tissue ChIP. We divided the proximal promoters of CaSR, TRPV6, VDR, CYP27B1, and CYP24 into 9 to 11 regions from the TSS or ATG to negative 5000 bp, and we designed the corresponding primers to amplify these regions. For the CaSR promoter regions, after administration of $1,25(OH)_2D_3$, the acetylated histone H3 increased only in region 10 and not in other regions compared to the vehicle treatment group (Fig. 4A). Histone modification within the intestinal TRPV6 promoter regions was strongly enhanced in regions 3, 4, and 6 (Fig. 4B). Furthermore, the modification of histone H3 within the VDR promoter in regions 1 and 7 was strongly enhanced by $1,25(OH)_2D_3$ treatment (Fig. 4C). Although a previous study showed that VDR only binds to two introns within the mouse VDR gene *in vitro*,[31] our data show that $1,25(OH)_2D_3$ modifies histone H3 at several VDR promoter regions. For the CYP27 promoter, since this gene was strongly inhibited after $1,25(OH)_2D_3$ administration (Fig. 4D), we investigated histone k9 methylation. Figure 4D shows that histone H3 methylation slightly increased in regions 1, 2, 3, and 4 in the $1,25(OH)_2D_3$ treatment group. For the CYP24 gene, we

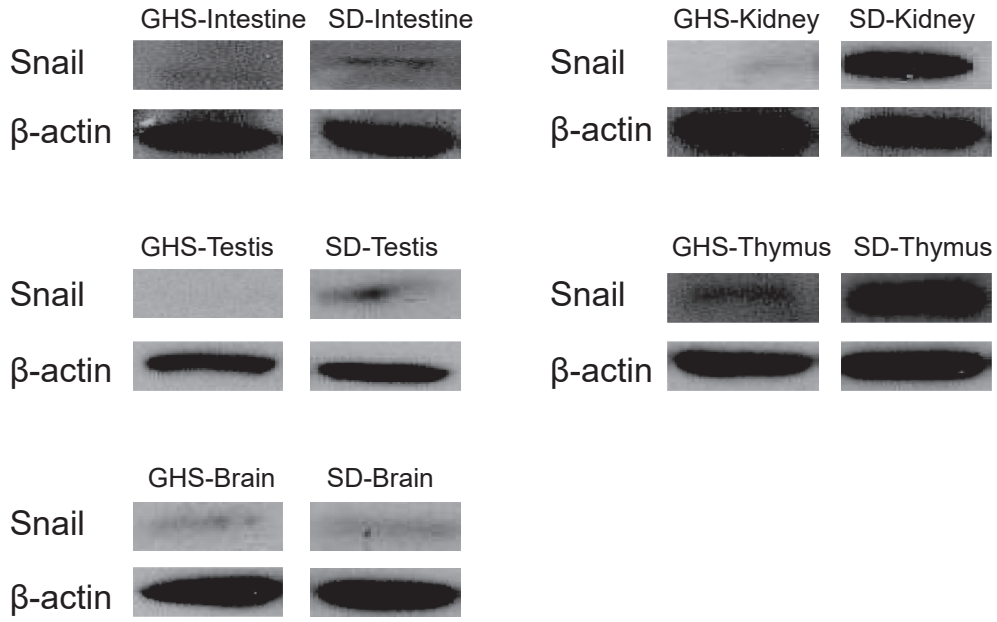

Figure 2 Snail expression in various tissues of GHS and SD rats. Nuclear proteins were isolated from tissues of three GHS rats and SD rats and then were subjected to Western blots using anti- Snail antibodies. Representative data are shown in Figure 2. Snail expression patterns were detected in GHS and SD rat tissues, and Snail expression was low in the intestine, kidney, thymus, and testis of GHS rats compared to SD rats.

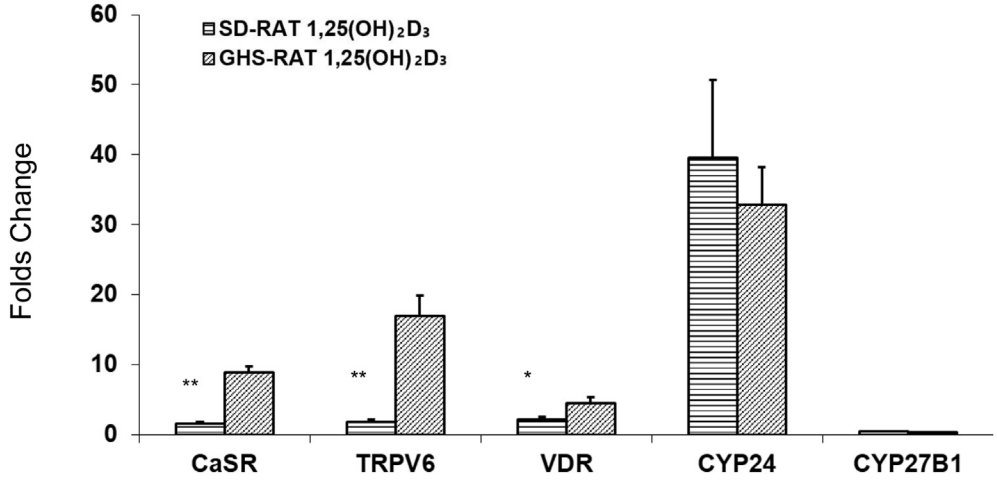

Figure 3 VDR target gene expression followed the administration of $1,25(OH)_2D_3$ in SD and GHS rats. Twelve hours after $1,25(OH)_2D_3$ treatment, kidney and intestine RNA was isolated and subjected to real-time PCR using specific primers for CaSR, TRPV6, VDR, CYP24, and CYP27. $1,25(OH)_2D_3$ upregulates CaSR, TRPV6, VDR, and CYP24 transcription and inhibits CYP27 transcription. Data are shown as the mean ± SEM, and the relative expression of target genes of the $1,25(OH)_2D_3$ treatment groups was normalized to the levels of the vehicle treatment groups.

found that $1,25(OH)_2D_3$ could change histone 3 acetylation in regions 1, 2, 5 and 8 (Fig. 4E).

VDR binds to multiple target gene promoter regions with histone modifications in GHS rats

VDR regulates target gene expression by recruiting coregulators and modifying the histone state.[25,30] To determine whether VDR regulates target gene expression through binding to promoter regions with histone modifications, quantitative tissue ChIP was performed on GHS rats that were treated with either a vehicle or $1,25(OH)_2D_3$. For the CaSR promoter, we screened 10 regions for VDR binding. We only found that VDR binds to region 10 when there was a histone modification after $1,25(OH)_2D_3$ injection (Fig. 4A). For the TRPV6 promoter, VDR binds to regions 3, 4, and 6 after $1,25(OH)_2D_3$ treatment (Fig. 4B). VDR accumulated in VDR promoter regions 1 and 7 when there were histone modifications after $1,25(OH)_2D_3$ administration (Fig. 4C). Previous data reported that

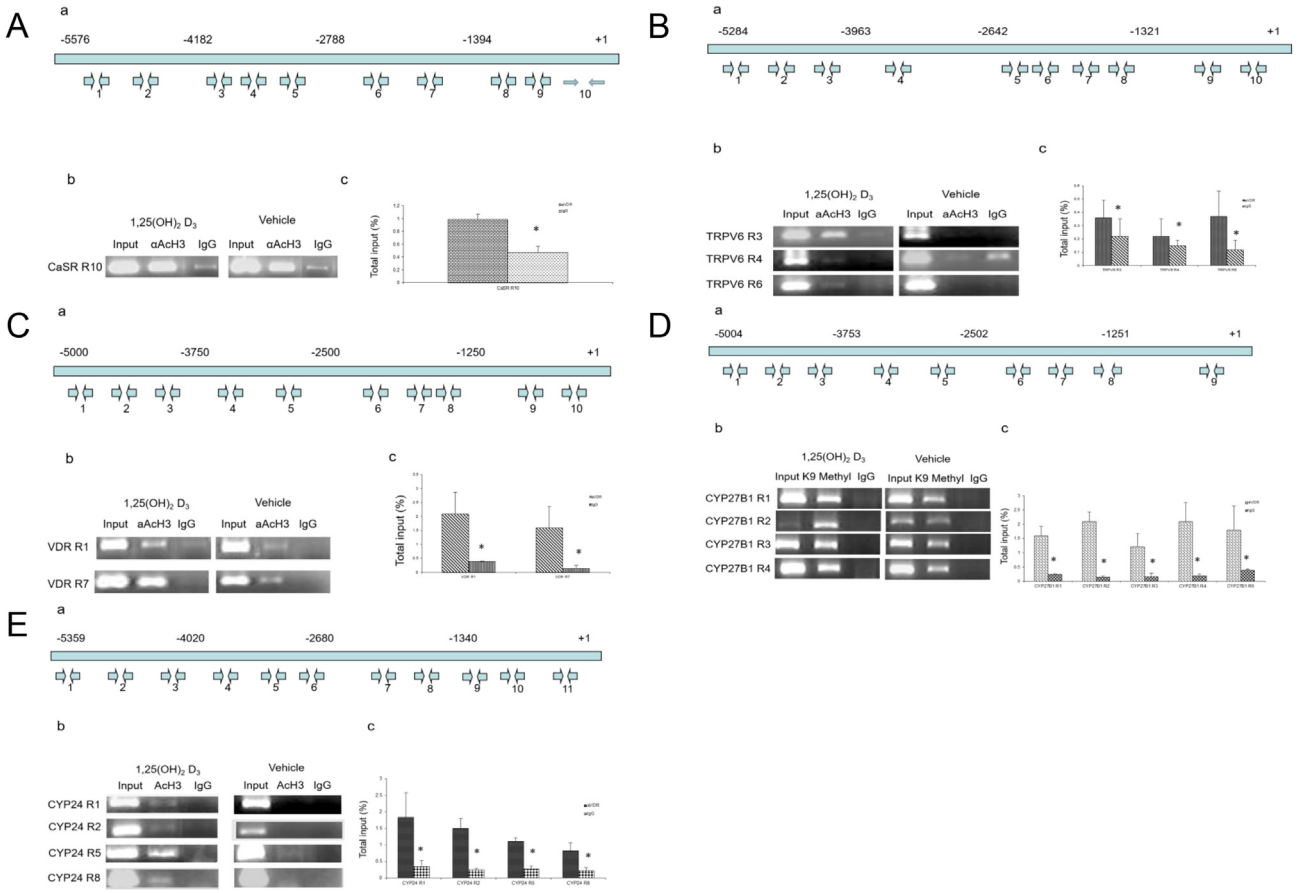

Figure 4 VDR binds to multiple promoter regions of its target genes and modifies histone 3. Four hours after $1,25(OH)_2D_3$ or vehicle treatment, the GHS rat intestines and kidneys were harvested and subjected to quantitative tissue ChIP. The data show real-time PCR results of input and DNA precipitated with anti-VDR or normal IgG using different region-specific primers (Table 1). Each group had at least three GHS rats, data are shown as the mean + SEM, and $P < 0.05$ was considered to be statistically significant. GHS rats were treated with $1,25(OH)_2D_3$ and vehicle. Twelve hours later, the kidney and intestine tissues were harvested and subjected to ChIP assays. Specific antibodies against acetylated and methylated histone H3 were used to precipitate the DNA. Primers as listed in Table 1 were used to amplify the different regions of target gene promoters. PCR products were run on a 2% agarose gel. **(A)** shows that VDR binds to CaSR promoter region 10 and modifies histone 3 acetylation in those region. **(B)** shows that VDR binds to TRPV6 promoter regions 3, 4 and 6 and modifies histone 3 acetylation in those regions. **(C)** shows that VDR binds to VDR promoter regions 1 and 7 and modifies histone 3 acetylation in those regions. **(D)** shows that VDR binds to CYP27 promoter regions 1, 2, 3 and 4 and modifies histone 3 K9 methylation in those regions. **(E)** shows that VDR binds to CYP24 promoter regions 1, 2, 5 and 8 and modifies histone 3 acetylation in those regions.

$1,25(OH)_2D_3$ could automatically upregulate VDR transcription through two enhancers within introns.[31] We next explored the localization of VDR at the CYP27B1 promoter after $1,25(OH)_2D_3$ treatment. Our data show that VDR binds to regions 1, 2, 3, 4, and 6. Interestingly, methylated histone H3 was slightly increased after $1,25(OH)_2D_3$ injection in the same regions (Fig. 4D). For the CYP24 promoter, VDR accumulated in regions 1, 2, 5, and 8 following $1,25(OH)_2D_3$ treatment (Fig. 4E). Taken together, our *in vivo* data strongly show that $1,25(OH)_2D_3$ induced or suppressed gene expression through VDR binding and histone modification.

Discussion

GHS rats resulted from breeding male and female SD rats with spontaneous hypercalciuria.[1] The high VDR levels in intestine, kidney, and bone cells can explain the hypercalciuria in GHS rats.[4–6] In this study, we explored whether VDR is highly expressed in all VDR-positive tissues. Our results show that VDR is highly expressed in the intestine and kidney, as previously reported,[4,7,8] which indicates that the high VDR in such tissues plays very important roles in defective Ca metabolism in GHS rats (Fig. 1). VDR is an essential nuclear receptor functioning in Ca metabolism, cell proliferation and differentiation in multiple tissues.[12–14] We also found that VDR is highly expressed in the prostate and thymus (Fig. 1), but the function of high VDR levels in such tissues remains unknown. Current studies show that Snail is a transcriptional repressor of VDR expression. Snail downregulates VDR expression through promoter binding, corepressor recruitment, and histone modification.[11] More importantly, Snail mRNA and protein levels are inversely correlated with those of VDR in GHS rats.[11] These results indicate that Snail is one of the essential regulators of high VDR expression in GHS rats. In

this study, we investigated Snail expression patterns in various tissues. Our results show that Snail is detectable in a few tissues in SD rats, such as the intestine, kidney, thymus, and testis, but it is absent or weakly expressed in GHS rats, which means that Snail is downregulated in tissues with high VDR expression in GHS rats (Fig. 2). Snail expression was not different between GHS and SD rat brains (Fig. 2). Interestingly, VDR expression also showed no difference in brains from GHS and SD rats (Fig. 1). Therefore, Snail and VDR are inversely expressed in rats, which may account for the higher VDR expression in GHS rats. The reason behind the low expression of Snail in GHS rats requires further study.

VDR-dependent gene regulation is a complex process involving promoter binding, coregulator recruitment, histone modification, and activation of the RNA pol II complex.[24,25] CYP24 and CYP27B1 are two vitamin D metabolizing enzymes and direct target genes of VDR. However, the mechanism by which $1,25(OH)_2D_3$ up- or downregulates CYP24 and CYP27B1 expression in a disease model has never been reported. In this study, 12 h after $1,25(OH)_2$ D_3 treatment of GHS rats, the mRNA levels of CYP24 and CYP27B1 dramatically increased by approximately 40-fold and decreased by approximately 70% ($P < 0.01$), respectively. Previous studies have found that $1,25(OH)_2$ D_3 levels correlate negatively or positively with kidney CYP24 and CYP27B1 levels.[15,33] Therefore, our results indicate that VDR maintains the normal $1,25(OH)_2D_3$ level in GHS rats through up- or downregulation of CYP24 and CYP27B1 gene expression. We also found that VDR upregulates CYP24 expression by binding to promoter regions 1, 2, 5, and 8 (approximately −5 kb, −4.5 kb, −2.5 kb, −1.5 kb and −0.5 kb upstream of the TSS) and subsequently hyperacetylates histone H3 in those regions (Fig. 4E). Previous *in vitro* data show that there are two VDREs within the proximal rat CYP24 promoter that mediate $1,25(OH)_2D_3$-activated *CYP24* gene transcription. The first one is located from −262 to −238 bp, and the second one is located from −154 to −134 bp.[19] Furthermore, we found that VDR binds to other proximal and distal promoter regions and changes histone acetylation in those regions. These results suggest that there may be multiple VDR binding sites within the rat CYP24 promoter. Histone methylation is an event associated with repression of gene expression.[32–34] Our *in vivo* data show that after $1,25(OH)_2D_3$ treatment, VDR binds to multiple regions of CYP27B1, regions 1, 2, 3, 4, and 6 (approximately −5 kb, −4.5 kb, −4 kb, −3 kb and −2.5 kb upstream of ATG, respectively), and it binds to slightly hypermethylated histone H3 at the same regions (Fig. 4D). Previous *in vitro* studies have indicated that VDR binds to multiple regions of the human CYP27B1 promoter and mediates transcriptional repression.[18] Our *in vivo* ChIP results indicate that VDR binds to rat CYP27B1 promoter regions 1, 2, 3, 4, and 6, which is consistent with Turunen's studies on the human CYP27B1 promoter.[18]

TRPV6 is an epithelial channel that is mainly expressed in the intestine.[22] The targeted distribution of TRPV6 in mice results in a 60% decrease in intestinal absorption, loss of bone mineral density, and lower fertility, which indicates that TRPV6 plays a central role in intestinal Ca absorption and whole-body Ca homeostasis.[23] GHS rats exhibit intestinal Ca hyperabsorption, which partially results from high levels of VDR, 8-kDa and 28-kDa calbindin, and CaSR in the intestine and kidney.[1,7–9] In this study, we investigated how elevated VDR upregulates TRPV6 expression in the intestines of GHS rats. After $1,25(OH)_2D_3$ treatment, TRPV6 mRNA increased approximately 15-fold compared to the vehicle group (Fig. 3), indicating that the TRPV6 gene is very sensitive to $1,25(OH)_2D_3$ stimuli. Therefore, the elevated VDR in GHS rats may upregulate TRPV6 expression, which contributes to intestinal Ca hyperabsorption. To date, very few studies have been performed on the mechanism of how $1,25(OH)_2D_3$ regulates rat TRPV6 gene expression *in vivo*. Our tissue ChIP results show that VDR quickly binds to multiple TRPV6 promoter regions, 3, 4, and 6 (approximately −4 kb, −3 kb, and −2 kb upstream of the TSS, respectively), which is followed by histone acetylation at the same regions and results in remarkable activation of *TRPV6* gene transcription (Fig. 4B). Pike's group investigated VDREs in human and mouse TRPV6 promoters *in vitro* and *in vivo*.[17,35] Their results show that the active VDREs in the human TRPV6 promoter are located at −4.3 and −2.1 kb relative to the TSS, and the mouse VDREs in the TRPV6 promoter are located at −2 and −4 kb relative to the TSS. Collectively, these data, together with our *in vivo* results, indicate that there may be some VDR binding sites in human, mouse, and rat TRPV6 promoter regions.

In vitro studies have revealed that $1,25(OH)_2D_3$ can directly modulate VDR transcription. VDR binds to two enhancers located in two introns and mediates automatic activation of the mouse VDR gene.[31] Our previous *in vivo* data showed that $1,25(OH)_2D_3$ could dramatically upregulate VDR transcription and expression at the mRNA and protein levels in GHS rats.[7] In the present study, we found that VDR binds to distal and proximal rat VDR promoter regions 1 and 7 (approximately −5 kb and −3.5 kb upstream of the TSS, respectively), which is followed by hyperacetylation of histone H3 at the same regions (Fig. 4C). Renal CaSR plays an essential role in renal Ca reabsorption through a CaSR-responsive K-dependent voltage-gated chloride channel.[35,36] The activation of CaSR may decrease renal tubule Ca reabsorption and cause hypercalciuria through suppression of Ca-sensitive potassium channel activity.[8] Our previous data show that CaSR is highly expressed in GHS rats compared to normal SD rats and contributes to kidney stone-forming and hypercalciuria in GHS rats.[8] However, the detailed mechanisms underlying the VDR-mediated regulation of CaSR are not clear. Here, we found that VDR binds to the rat proximal CaSR promoter region 10, which is followed by hyperacetylation of histone H3. Another *in vitro* study on the human CaSR promoter reported that VDR binds to the same region within the human CaSR promoter.[21] Taken together, these results indicate that there may be potential VDREs in the rat CaSR proximal promoter region.

Conclusion

In summary, our studies indicate that the elevation of VDR up- or downregulates target genes associated with vitamin D metabolism and Ca homeostasis by binding to multiple promoter regions and hyperacetylating or

hypermethylating histone H3. These *in vivo* data provide deep insights into how VDR regulates rat target gene expression *in vivo*.

Conflict of interests

There are no interests conflict.

Acknowledgements

The research is supported by the hospital's own funds (ynlc201721).

Appendix A. Supplementary data

Supplementary data to this article can be found online at https://doi.org/10.1016/j.gendis.2020.09.001.

References

1. Favus MJ. Hypercalciuria: lessons from studies of genetic hypercalciuric rats. *J Am Soc Nephrol*. 1994;5:S54—S58.
2. Bushinsky DA, Favus MJ. Mechanism of hypercalciuria in genetic hypercalciuric rats. Inherited defect in intestinal calcium transport. *J Clin Invest*. 1988;82:1585—1591.
3. Pak CY, Oata M, Lawrence EC, Snyder W. The hypercalciurias. Causes, parathyroid functions, and diagnostic criteria. *J Clin Invest*. 1974;54:387—400.
4. Li XQ, Tembe V, Horwitz GM, Bushinsky DA, Favus MJ. Increased intestinal vitamin D receptor in genetic hypercalciuric rats. A cause of intestinal calcium hyperabsorption. *J Clin Invest*. 1993;91:661—667.
5. Krieger NS, Stathopoulos VM, Bushinsky DA. Increased sensitivity to $1,25(OH)_2D_3$ in bone from genetic hypercalciuric rats. *Am J Physiol*. 1996;271:C130—C135.
6. Tsuruoka S, Bushinsky DA, Schwartz GJ. Defective renal calcium reabsorption in genetic hypercalciuric rats. *Kidney Int*. 1997;51:1540—1547.
7. Yao J, Kathpalia P, Bushinsky DA, Favus MJ. Hyperresponsiveness of vitamin D receptor gene expression to 1,25-dihydroxyvitamin D3. A new characteristic of genetic hypercalciuric stone-forming rats. *J Clin Invest*. 1998;101:2223—2232.
8. Yao JJ, Bai S, Karnauskas AJ, Bushinsky DA, Favus MJ. Regulation of renal calcium receptor gene expression by 1,25-dihydroxyvitamin D3 in genetic hypercalciuric stone-forming rats. *J Am Soc Nephrol*. 2005;16:1300—1308.
9. Karnauskas AJ, Van Leeuwen JP, Van den Bemd GJ, et al. Mechanism and function of high vitamin D receptor levels in genetic hypercalciuric stone-forming rats. *J Bone Miner Res*. 2005;20:447—454.
10. Palmer HG, Larriba MJ, Garcia JM, et al. The transcription factor SNAIL represses vitamin D receptor expression and responsiveness in human colon cancer. *Nat Med*. 2004;10:917—919.
11. Bai S, Wang H, Shen J, Zhou R, Bushinsky DA, Favus MJ. Elevated vitamin D receptor levels in genetic hypercalciuric stone-forming rats are associated with downregulation of Snail. *J Bone Miner Res*. 2010;25:830—840.
12. Holick MF. Sunlight and vitamin D for bone health and prevention of autoimmune diseases, cancers, and cardiovascular disease. *Am J Clin Nutr*. 2004;80:1678S—1688S.
13. Holick MF. Resurrection of vitamin D deficiency and rickets. *J Clin Invest*. 2006;116:2062—2072.
14. Holick MF. Calcium plus vitamin D and the risk of colorectal cancer. *N Engl J Med*. 2006;354:2287—2288.
15. Anderson P, May B, Morris H. Vitamin D metabolism: new concepts and clinical implications. *Clin Biochem Rev*. 2003;24:13—26.
16. Zierold C, Darwish HM, DeLuca HF. Two vitamin D response elements function in the rat 1,25-dihydroxyvitamin D 24-hydroxylase promoter. *J Biol Chem*. 1995;270:1675—1678.
17. Meyer MB, Zella LA, Nerenz RD, Pike JW. Characterizing early events associated with the activation of target genes by 1,25-dihydroxyvitamin D3 in mouse kidney and intestine *in vivo*. *J Biol Chem*. 2007;282:22344—22352.
18. Turunen MM, Dunlop TW, Carlberg C, Vaisanen S. Selective use of multiple vitamin D response elements underlies the 1 alpha,25-dihydroxyvitamin D3-mediated negative regulation of the human CYP27B1 gene. *Nucleic Acids Res*. 2007;35:2734—2747.
19. Kerry DM, Dwivedi PP, Hahn CN, Morris HA, Omdahl JL, May BK. Transcriptional synergism between vitamin D-responsive elements in the rat 25-hydroxyvitamin D3 24-hydroxylase (CYP24) promoter. *J Biol Chem*. 1996;271:29715—29721.
20. Chikatsu N, Fukumoto S, Takeuchi Y, et al. Cloning and characterization of two promoters for the human calcium-sensing receptor (CaSR) and changes of CaSR expression in parathyroid adenomas. *J Biol Chem*. 2000;275:7553—7557.
21. Canaff L, Hendy GN. Human calcium-sensing receptor gene. Vitamin D response elements in promoters P1 and P2 confer transcriptional responsiveness to 1,25-dihydroxyvitamin D. *J Biol Chem*. 2002;277:30337—30350.
22. Perez AV, Picotto G, Carpentieri AR, Rivoira MA, Peralta Lopez ME, De Talamoni NGT. Minireview on regulation of intestinal calcium absorption. Emphasis on molecular mechanisms of transcellular pathway. *Digestion*. 2008;77:22—34.
23. Bianco SD, Peng JB, Takanaga H, et al. Marked disturbance of calcium homeostasis in mice with targeted disruption of the Trpv6 calcium channel gene. *J Bone Miner Res*. 2007;22:274—285.
24. Pike JW, Meyer MB, Watanuki M, et al. Perspectives on mechanisms of gene regulation by 1,25-dihydroxyvitamin D3 and its receptor. *J Steroid Biochem Mol Biol*. 2007;103:389—395.
25. Pike JW, Zella LA, Meyer MB, Fretz JA, Kim S. Molecular actions of 1,25-dihydroxyvitamin D3 on genes involved in calcium homeostasis. *J Bone Miner Res*. 2007;22:V16—V19.
26. Wang HW, Muguira M, Liu WD, et al. Identification of an INSM1-binding site in the insulin promoter: negative regulation of the insulin gene transcription. *J Endocrinol*. 2008;198:29—39.
27. Pfaffl MW. A new mathematical model for relative quantification in real-time RT-PCR. *Nucleic Acids Res*. 2001;29:e45.
28. Yu Z, Wang C, Wang M, et al. A cyclin D1/microRNA 17/20 regulatory feedback loop in control of breast cancer cell proliferation. *J Cell Biol*. 2008;182:509—517.
29. Thuault S, Tan EJ, Peinado H, Cano A, Heldin CH, Moustakas A. HMGA2 and Smads co-regulate SNAIL1 expression during induction of epithelial-to-mesenchymal transition. *J Biol Chem*. 2008;283:33437—33446.
30. Dusso AS. Vitamin D receptor: mechanisms for vitamin D resistance in renal failure. *Kidney Int Suppl*. 2003;63(S 85):S6—S9.
31. Zella LA, Kim S, Shevde NK, Pike JW. Enhancers located within two introns of the vitamin D receptor gene mediate transcriptional autoregulation by 1,25-dihydroxyvitamin D3. *Mol Endocrinol*. 2006;20:1231—1247.
32. Villeneuve LM, Reddy MA, Lanting LL, Wang M, Meng L, Natarajan R. Epigenetic histone H3 lysine 9 methylation in metabolic memory and inflammatory phenotype of vascular smooth muscle cells in diabetes. *Proc Natl Acad Sci U S A*. 2008;105:9047—9052.

33. Panda DK, Al Kawas S, Seldin MF, Hendy GN, Goltzman D. 25-hydroxyvitamin D 1alpha-hydroxylase: structure of the mouse gene, chromosomal assignment, and developmental expression. *J Bone Miner Res*. 2001;16:46—56.
34. Li Y, Reddy MA, Miao F, et al. Role of the histone H3 lysine 4 methyltransferase, SET7/9, in the regulation of NF-kappaB-dependent inflammatory genes. Relevance to diabetes and inflammation. *J Biol Chem*. 2008;283:26771—26781.
35. Meyer MB, Watanuki M, Kim S, Shevde NK, Pike JW. The human transient receptor potential vanilloid type 6 distal promoter contains multiple vitamin D receptor binding sites that mediate activation by 1,25-dihydroxyvitamin D3 in intestinal cells. *Mol Endocrinol*. 2006;20:1447—1461.
36. Wang WH, Lu M, Hebert SC. Cytochrome P-450 metabolites mediate extracellular Ca(2+)-induced inhibition of apical K+ channels in the TAL. *Am J Physiol*. 1996;271:C103—C111.